NOTICE: When government or other drawings, specifications or other data are used for any purpose other than in connection with a definitely related government procurement operation, the U. S. Government thereby incurs no responsibility, nor any obligation whatsoever; and the fact that the Government may have formulated, furnished, or in any way supplied the said drawings, specifications, or other data is not to be regarded by implication or otherwise as in any manner licensing the holder or any other person or corporation, or conveying any rights or permission to manufacture, use or sell any patented invention that may in any way be related thereto.

63-1-4

HUGHES TOOL COMPANY · AIRCRAFT DIVISION

Culver City, California

Report 285-14 (62-14)

CONTRACT NO. AF 33(600)-30271

HOT CYCLE ROTOR SYSTEM
ROTOR DYNAMICS

March 1962

HUGHES TOOL COMPANY -- AIRCRAFT DIVISION
Culver City, California

HUGHES TOOL COMPANY
AIRCRAFT DIVISION

For

Commander

Aeronautical Systems Division

Prepared by:

S. V. LaForge
Aeronautical Engineer

Approved by: K B Amer

K. B. Amer
Chief Helicopter
Research Engineer

J L Velazquez

J. L. Velazquez
Sr. Project Engineer

H. O. Nay

H. O. Nay
Manager, Transport Helicopter
Department

FOREWORD

This report has been prepared by Hughes Tool Company -- Aircraft Division under USAF Contract AF 33(600)-30271 "Hot Cycle Pressure Jet Rotor System", D/A Project Number 9-38-01-000, Subtask 616.

The Hot Cycle Pressure Jet Rotor System is based on a principle wherein the exhaust gases from high pressure ratio turbojet engine(s) located in the fuselage are ducted through the rotor hub and blades and are exhausted through a nozzle at the blade tips. Forces thus produced drive the rotor.

The objectives of this contract are to:

1. Analyze utility of the concept as applied to helicopters, compound helicopters, and convertiplanes of various sizes.
2. Demonstrate structural feasibility by design, fabrication and whirl test of a rotor (25 hours of whirl test).
3. Further explore rotor characteristics.
   a. Aerodynamic and Dynamic (additional 10 hours of whirl test)
   b. Endurance-type check (additional 25 hours of whirl test)
4. Study control problems involved in gas coupled engine and rotor.

This report covers that portion of the work pertaining to analysis of the design prior to whirl test, specifically a study of blade potential resonances. It is in partial fulfillment of Item 4e, covering Analysis Pertaining to Design of the Rotor System, performed under Item 4b of the contract.

TABLE OF CONTENTS

SUMMARY

Figure 1 presents the predicted blade elastic resonant conditions for the Hot Cycle whirl test rotor. This figure indicates the rotor should be free of resonance within the operating range.

The apparent resonance of chordwise cantilever second mode with a 6/rev exciting force in the operating range of RPM is not expected to occur. This is because the exciting forces are assumed of aerodynamic origin and, in a 3-bladed rotor, 6/rev aerodynamic forces will excite chordwise pinned modes only.

METHOD OF ANALYSIS

The Myklestad method of determining the theoretical natural frequencies was used. A discussion of this method is presented in the Appendix. The Myklestad analysis was programed on the IBM 7090 computer. The analysis uses 21 stations and determines the natural frequency to within .001 rad/sec.

The natural frequency occurs when the bending moment at the root is zero on a pinned free blade (flapwise bending) and when the angle at the root is zero for a fixed free blade (chordwise cantilever bending).* Thus, it is necessary to compute the root moment or angle at various frequencies (ω) to determine the resonance point. This was done by starting at $\omega = 1.2$ x rotor speed and increasing ω until the root moment or angle changes sign. After a change in sign occurs, a parabola is passed through the last three points to determine the next try for ω. This is done until ω converges to within .001 rad/sec. The mode shape is then determined for this resonant frequency. The program continues increasing ω and searching for the resonant frequencies until four modes are obtained.

It is known that, approximately

$$\omega^2_{rot} = \omega^2_{non\text{-}rot} + k\Omega^2 \qquad (1)$$

where ω_{rot} = the natural frequency of the rotating blade

$\omega_{non\text{-}rot}$ = the non-rotating natural frequency of the blade

Ω = rotating frequency of the rotor

k = a numerical factor which differs for each mode.

* See Figure 2 for mode shapes.

The theoretical value of k was obtained from the Myklestad analysis described above. This was done for all bending modes of Figure 1 with the exception of the chordwise cantilever second mode which was developed from an Yntema analysis, Reference 1.

Then, from shake test results*, the actual value (or in most cases range of values) for $\omega_{\text{non-rot}}$ was determined. These values were reduced by a factor $\sqrt{\dfrac{14 \times 10^6}{16 \times 10^6}}$ which is meant to account approximately for the reduction of the modulus of elasticity of the titanium spars from the room temperature value at which the shake tests were performed to the value when the spars are at whirl test operational temperatures.

Having then established $\omega_{\text{non-rot}}$, the value of k determined as described above was assumed to be valid for the actual blade. Under these conditions, the frequency lines of Figure 1 were plotted.

The measured chordwise cantilever frequencies were corrected for the tension load applied to prevent buckling of the straps.

The chordwise pin-end mode was corrected from the test condition (pinned at the feathering ball) to the operational condition (pinned at the rotor shaft).

The third mode flapwise frequency curve is based entirely on theoretical calculations inasmuch as the shake tests were not carried out to high enough frequency to excite the non-rotating third mode flapwise frequency.

* Reference 2

DISCUSSION

Table 1 presents the predicted Hot Cycle Resonances between 70% and 99% of Minimum Normal Operating Rotor RPM. These values were obtained from Figure 1

Table I

Predicted Hot Cycle Resonances Between

70% and 99% of Minimum Normal Operating Rotor RPM

Subsystem	Natural Frequency Ratio (per rev) At Resonance	Rotor RPM At Resonance	% Minimum Normal Operating RPM	Remarks
Flapwise 2nd Mode	5/rev	151-193	72-88	
Flapwise 3rd Mode	7/rev	205	94	
Chordwise Cantilever 1st Mode	2/rev	175	80	
Chordwise Pinned 1st Mode	6/rev	197	90	
Chordwise Cantilever 2nd Mode	7/rev	188-197	86-90	
	8/rev	164-172	75-78	

Elastic Flapwise Modes

1st Mode Flapwise - The predicted natural frequency ratio squared as a function of rotor rpm squared is shown in Figure 1.

At about 85 rpm, the natural frequency ratio is 3/rev. Thereafter, as rotor speed increases, the frequency ratio moves toward 2/rev and farther away from a multiple of rotor speed. There appears to be no problem in this mode.

<u>2nd Mode Flapwise</u> - The second mode flapwise natural frequency is also shown in Figure 1. The natural frequency ratio passes through 6/rev, and higher resonances below 139 rpm. The range of possible second mode flapwise resonance with 5/rev indicates a possibility of resonance as high as 193 rpm (88% of the minimum operating rpm).

<u>3rd Mode Flapwise</u> - The predicted third mode flapwise resonance also appears in the figures. This prediction is less reliable than the lower modes since there were no attempts during shake tests to find a stationary third mode frequency. A 7/rev resonance at 205 rpm (94% of minimum rpm) is indicated.

<u>Elastic Chordwise Modes</u>

For chordwise elastic vibration there exist two possible end conditions at the centerline of rotation. The end condition depends on whether the elastic motions of the three blades are in phase or out of phase. If all three blade motions are in phase, then the center of rotation behaves as a pinned beam. For aerodynamic forcing, the pinned end condition should occur at 3/rev, 6/rev, 9/rev, etc.

If the blade motions are opposed to one another, then the center of rotation behaves as a fixed beam. Aerodynamic forcing for fixed root modes should occur at all multiples of rotor speed

except integer multiples of the total number of blades (in this case, 3).

1st Mode Chordwise Pinned - At rotor speeds less than normal operating rpm, 1st mode chordwise pinned should be in resonance with 9/rev at 125 rpm and 6/rev at 197 rpm. This latter value is 90% of minimum normal operating rpm.

No higher modes of chordwise pinned are considered since they will be of quite high frequency and are unsubstantiated by any shake tests.

First Mode Chordwise Cantilever - As seen in Figure 1, the slope of the plot of first mode chordwise cantilever is small and the value of frequency is rather low. Thus, the frequency plot crosses all the per rev lines except 1/rev below operating rpm. At 175 rpm, this mode is in resonance with a 2/rev force. In the operating range, the frequency appears to be adequately below 2/rev and above 1/rev.

Second Mode Chordwise Cantilever - This frequency plot is intercepted by a 6/rev line in the operating range of rpm. However, if it is assumed all forcing functions for this mode are of aerodynamic origin, then any 6/rev harmonic would excite a pin-ended mode and not a fixed ended mode. On this basis it is assumed no serious resonance with 6/rev forces will occur for this mode.

Resonance with 7/rev or 8/rev harmonics of an aerodynamic exciting force are possible, however. Resonance with 7/rev for second mode cantilever is possible at 197 rpm as seen in Figure 1. This is 90% of minimum normal operating rpm.

REFERENCES

1. Yntema, Robert T., "Rapid Estimation of Bending Frequencies of Rotating Beams", NACA RM L54602, 1954.

2. "Results of Component Test Program Hot Cycle Rotor System", Final Report, Item 6a, March 1962, Report No. 285-9-8, (62-8).

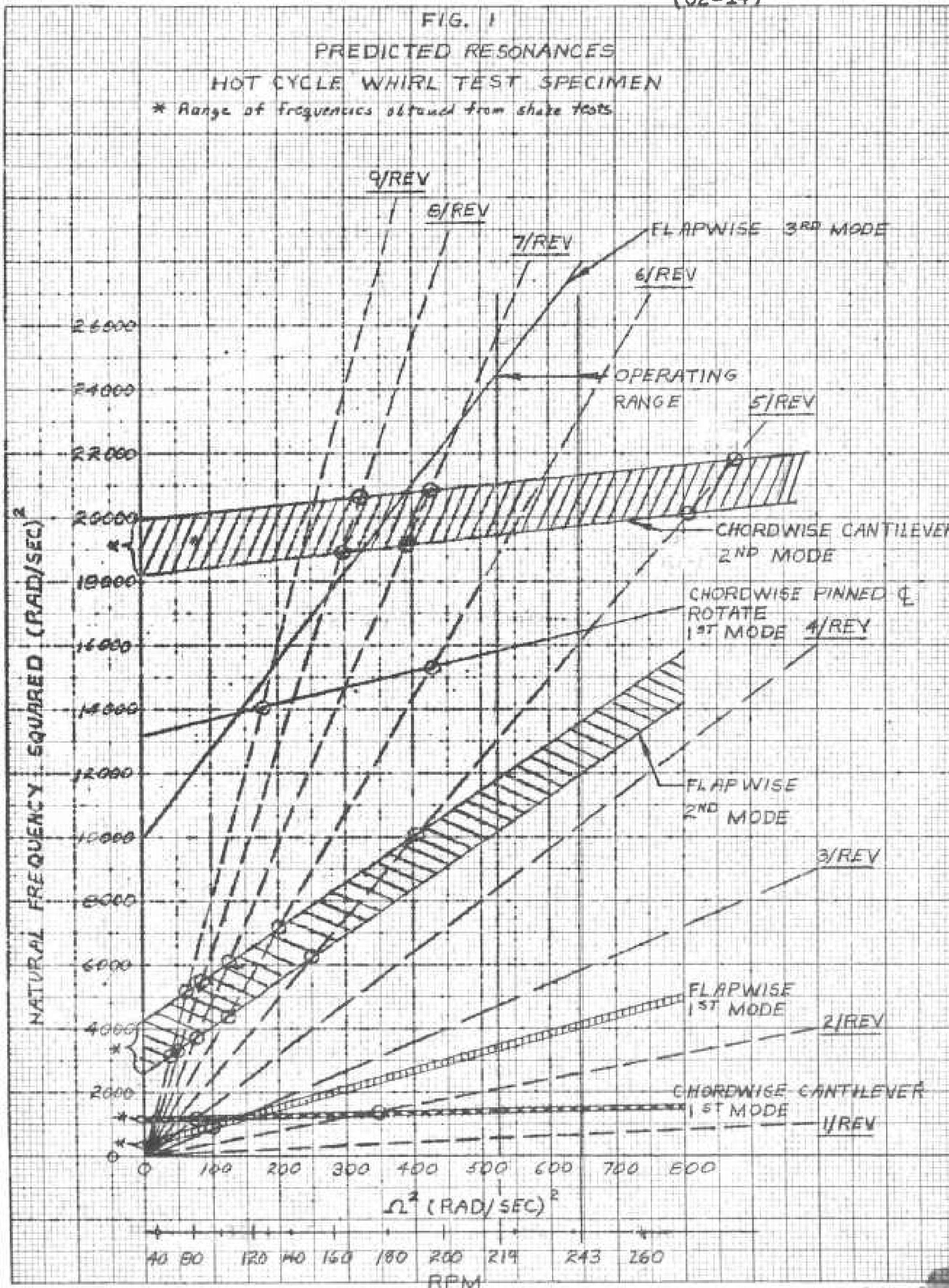
FIG. 1
PREDICTED RESONANCES
HOT CYCLE WHIRL TEST SPECIMEN
* Range of frequencies obtained from shake tests
9/REV
8/REV
7/REV
6/REV
5/REV
4/REV
3/REV
2/REV
1/REV
FLAPWISE 3RD MODE
OPERATING RANGE
CHORDWISE CANTILEVER 2ND MODE
CHORDWISE PINNED ℄ ROTATE 1ST MODE
FLAPWISE 2ND MODE
FLAPWISE 1ST MODE
CHORDWISE CANTILEVER 1ST MODE
NATURAL FREQUENCY SQUARED (RAD/SEC)²
26000
24000
22000
20000
18000
16000
14000
12000
10000
8000
6000
4000
2000
0
0 100 200 300 400 500 600 700 800
Ω² (RAD/SEC)²
40 80 120 140 160 180 200 219 243 260
RPM

3-5-62

Figure 2

Hot Cycle Blade Mode Shapes

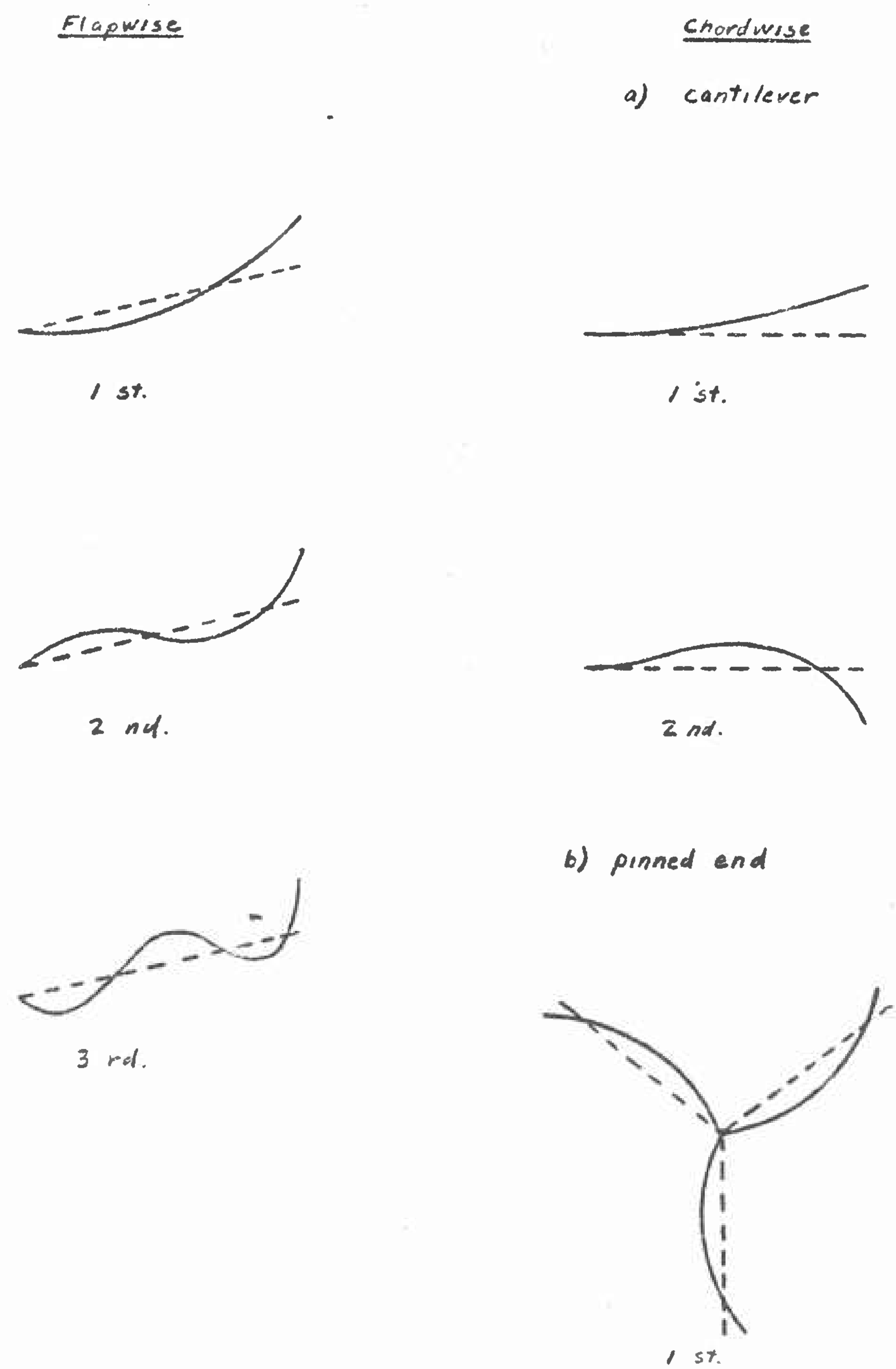

APPENDIX A

Natural Frequencies and Mode Shapes Of A Rotor Blade Including Shear Deflections And Rotary Inertia By The Myklestad Method

SYMBOLS FOR APPENDIX A

A	=	Cross section area.
CF	=	Centrifugal force.
d_F	=	Deflection due to shear, see Figure 3.
d_M	=	Deflection due to moment, see Figure 2.
E	=	Modulus of elasticity,
e	=	Hinge offset.
G	=	Modulus of rigidity.
H	=	Lumped mass moment of inertia.
I	=	Cross section area moment of inertia.
IF	=	Inertia force.
IM	=	Inertia moment.
K	=	Constant depending on shape of cross section, see equation 1.
L	=	Length of blade segment, see Figure 1.
ℓ	=	Distance between lumped masses, see Figure 1.
M	=	Moment.
m	=	Lumped mass, see Figure 1.
r	=	Distance from centerline to section of blade, see Figure 1.
S	=	Shear
V_F	=	Slope due to shear, see Figure 3.
V_M	=	Slope due to moment, see Figure 2.

X = Distance from hinge to section of blade, see Figure 1.

y = Deflection.

α = Slope.

Ω = Rotor angular velocity.

ω = Natural frequency.

<u>Subscripts</u>

i = Refers to station.

R.E.H.

Natural Frequencies and Mode Shapes of a Rotor Blade Including Shear Deflections and Rotary Inertia by the Myklestad Method

The following pages contain the derivation of the equations required for the determination of the natural frequencies and mode shapes of a rotor blade. The recursion expressions for shear, moment, slope and deflection are obtained. These equations are also written using matrix notation. The recursion equations are

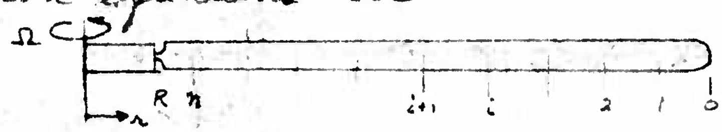

$$S_{i+1} = [1+\omega^2 m_{i+1} D_{F_i} + \Omega^2 a_{i+1} V_{F_i}]\, S_i + [\omega^2 m_{i+1} D_{M_i} + \Omega^2 a_{i+1} V_{M_i}]\, M_i + m_{i+1}[-\omega^2 l_i - \Omega^2 r_{i+1}]\,\alpha_i + [\omega^2 m_{i+1}]\, y_i$$

$$M_{i+1} = [l_i - \omega^2 H_{i+1} V_{F_i} + \Omega^2 a_i D_{F_i}]\, S_i + [1 - \omega^2 H_{i+1} V_{M_i} + \Omega^2 a_i D_{M_i}]\, M_i + [\omega^2 H_{i+1}]\,\alpha_i$$

$$\alpha_{i+1} = -V_{F_i} S_i - V_{M_i} M_i + \alpha_i$$

$$y_{i+1} = D_{F_i} S_i + D_{M_i} M_i - l_i \alpha_i + y_i$$

or using matrix notation they can be written as

$$\begin{Bmatrix} S \\ M \\ \alpha \\ y \end{Bmatrix}_{i+1} = \begin{bmatrix} a_{11} & a_{12} & a_{13} & a_{14} \\ a_{21} & & - & - \\ \vdots & & & \\ a_{41} & - & - & a_{44} \end{bmatrix}_i \begin{Bmatrix} S \\ M \\ \alpha \\ y \end{Bmatrix}_i$$

or more compactly as

$$C_{i+1} = A_i C_i$$

R.E.H. ①

Natural Frequencies and Mode Shapes of a Rotor Blade Including Shear Deflections and Rotary Inertia by the Myklestad Method

This note contains the derivation of the recurrence formulas involved in the determination of rotor blade natural frequencies and modes shapes including shear deflections and rotatory inertia. The derivation will first consider the case of flapwise bending, and then it will be shown that the same equations can be used for chordwise bending by making a simple transformation.

The method consists of first replacing the distributed system by a lumped parameter system. Then the aim is to express the shear, moment, slope and deflection at one station in terms of the same quantities at the adjacent station. By repeatedly applying these relations the shear, moment, slope and deflection at one end of the rotor blade can be expressed in terms of the same quantities at the other end. The notation used in the lumped parameter system is illustrated in Figure 1.

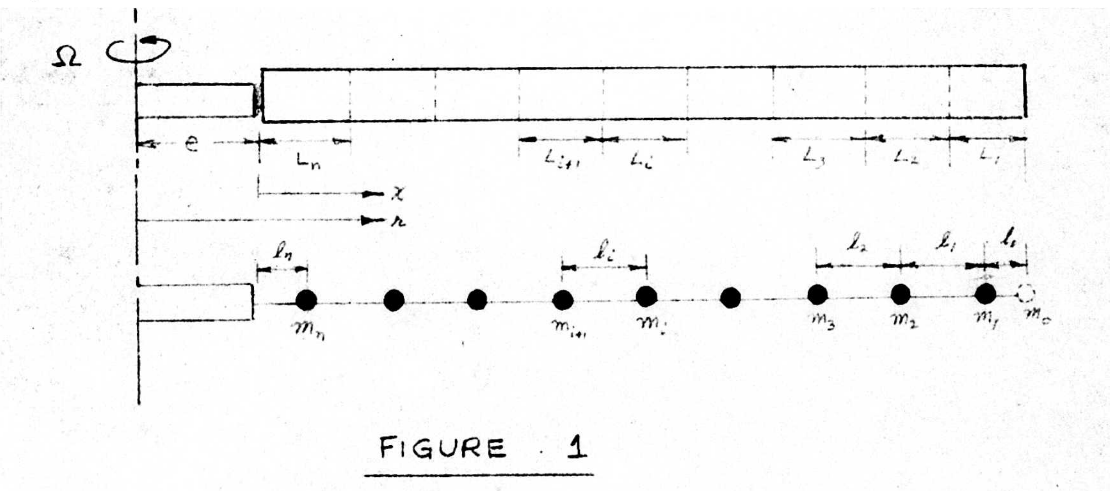

FIGURE 1

It is assumed that there is a zero mass, m_o, at the free end of the rotor blade. This zero mass is added so that the length of the lumped parameter blade will be equal to the actual blade length and so that the shear at the free end will be zero as it should be.

The change in slope and deflection between any two stations depends on the elastic properties of the blade as well as the shear and moment. This change in slope and deflection will be determined using the Timoshenko beam theory. This theory includes the deflections due to shear distorsions as well as the deflection due to bending. As the shear distorsion involves a sliding of adjacent fibers the bending angle will not be affected. The elastic parameters which will be used in the derivation are illustrated in Figures 2 and 3.

FIGURE 2 DEFLECTION AND SLOPE DUE TO A UNIT MOMENT

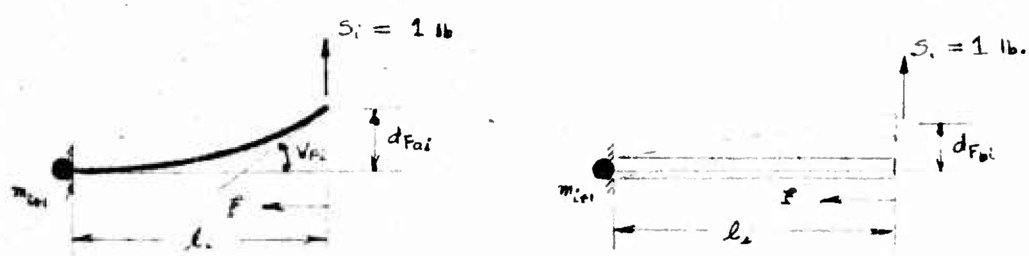

3a BENDING EFFECT

3b SHEAR EFFECT

FIGURE 3 DEFLECTION AND SLOPE DUE TO A UNIT SHEAR

From the area moment principle the elastic coefficients are given by

$$\left.\begin{aligned} v_{M_i} &= \int_0^{l_i} \frac{d\xi}{EI} & \qquad v_{F_i} = d_{M_i} &= \int_0^{l_i} \frac{\xi\, d\xi}{EI} \\ d_{Fai} &= \int_0^{l_i} \frac{\xi^2\, d\xi}{EI} & \qquad d_{Fbi} &= \int_0^{l_i} \frac{d\xi}{KAG} \end{aligned}\right\} \quad (1)$$

where K is a factor depending on the shape of the cross section. Roark gives values of K of 9/10 for a solid circular section and 1/2 for a thin-walled hollow circular section. For a beam with constant properties over the length l_i these expressions become

$$\left.\begin{aligned} v_{M_i} &= \left(\frac{l}{EI}\right)_i & \qquad v_{F_i} = d_{M_i} &= \frac{1}{2}\left(\frac{l^2}{EI}\right)_i \\ d_{Fai} &= \frac{1}{3}\left(\frac{l^3}{EI}\right)_i & \qquad d_{Fbi} &= \left(\frac{l^3}{KAG}\right)_i \end{aligned}\right\} \quad (2)$$

Let us define the deflection due to a unit shear by d_{F_i}, i.e.

$$d_{F_i} = d_{Fai} + d_{Fbi} \qquad (3)$$

Figure 4 illustrates a free body diagram of the i^{th} segment when it is vibrating at the natural frequency ω and the rotor is turning at the speed Ω. H_i is the lumped mass moment of inertia of the i^{th} segment.

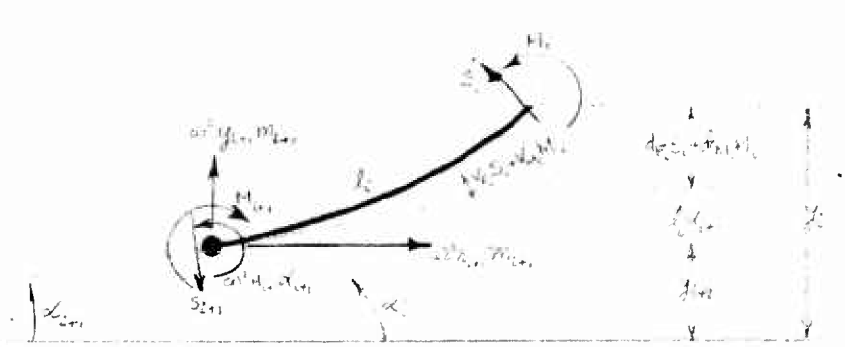

FIGURE 4 FREE BODY DIAGRAM OF BLADE SEGMENT

Referring to Figure 4 we obtain the following relations between the slope and deflection at each end of the segment

$$\boxed{\alpha_{i+1} = -V_{F_i} S_i - V_{M_i} M_i + \alpha_i} \qquad (4)$$

$$y_{i+1} = -d_{F_i} S_i - d_{M_i} M_i - l_i \alpha_{i+1} + y_i$$

$$= -d_{F_i} S_i - d_{M_i} M_i - l_i \left[-V_{F_i} S_i - V_{M_i} M_i + \alpha_i \right] + y_i$$

$$\boxed{y_{i+1} = D_{F_i} S_i + D_{M_i} M_i - l_i \alpha_i + y_i} \qquad (5)$$

where

$$\left.\begin{aligned} D_{F_i} &= l_i V_{F_i} - d_{F_i} \\ D_{M_i} &= l_i V_{M_i} - d_{M_i} \end{aligned}\right\} \qquad (6)$$

In order to obtain the shear and moment relations refer to Figure 5 where

$(I.F.)_i$ = inertia force = $\omega^2 y_i m_i$

$(I.M.)_i$ = inertia moment = $\omega^2 \alpha_i H_i$

$(C.F.)_i$ = centrifugal force = $\Omega^2 r_i m_i$

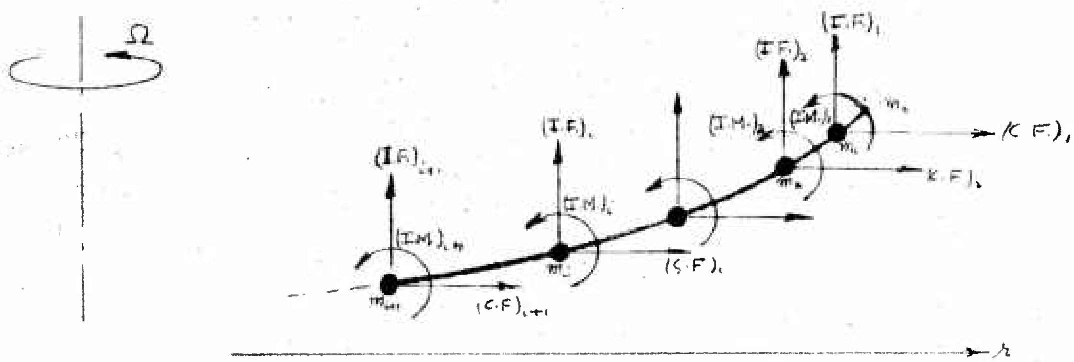

FIGURE 5 EXTERNAL FORCES ACTING ON THE RIGHT HAND SECTION

From Figure 5 the shear at the i+1 and i stations can be written as

$$\left.\begin{aligned} S_{i+1} &= \sum_{j=0}^{i+1} \omega^2 m_j y_j - \alpha_{i+1} \sum_{j=0}^{i+1} \Omega^2 m_j r_j \\ S_i &= \sum_{j=0}^{i} \omega^2 m_j y_j - \alpha_i \sum_{j=0}^{i} \Omega^2 m_j r_j \end{aligned}\right\} \qquad (7\,a,b)$$

Subtracting S_i from S_{i+1} yields

$$S_{i+1} - S_i = \omega^2 m_{i+1} y_{i+1} - \alpha_{i+1} m_{i+1} r_{i+1} \Omega^2 - (\alpha_{i+1} - \alpha_i) \sum_{j=0}^{i} \Omega^2 m_j r_j$$

$$= \omega^2 m_{i+1} y_{i+1} - \Omega^2 a_{i+1} \alpha_{i+1} + \Omega^2 \alpha_i a_i \qquad (8)$$

where we have written

$$a_i = \sum_{j=0}^{i} m_j r_j \qquad (9)$$

Introducing (4) and (5) into (8) results in

$$S_{i+1} - S_i = \omega^2 m_{i+1} \left[D_{F_i} S_i + D_{M_i} M_i - l_i \alpha_i + y_i \right] - \Omega^2 a_{i+1} \left[-V_{F_i} S_i - V_{M_i} M_i + \alpha_i \right] + \Omega^2 \alpha_i a_i$$

$$S_{i+1} = \left[1 + \omega^2 m_{i+1} D_{F_i} + \Omega^2 a_{i+1} V_{F_i} \right] S_i + \left[\omega^2 m_{i+1} D_{M_i} + \Omega^2 a_{i+1} V_{M_i} \right] M_i - \left[\omega^2 m_{i+1} l_i + \Omega^2 a_{i+1} - \Omega^2 a_i \right] \alpha_i + \omega^2 m_{i+1} y_i$$

or finally

$$\boxed{S_{i+1} = \left[1 + \omega^2 m_{i+1} D_{F_i} + \Omega^2 a_{i+1} V_{F_i} \right] S_i + \left[\omega^2 m_{i+1} D_{M_i} + \Omega^2 a_{i+1} V_{M_i} \right] M_i + m_{i+1} \left[-\omega^2 l_i - \Omega^2 r_{i+1} \right] \alpha_i + \omega^2 m_{i+1} y_i} \qquad (10)$$

From Figure 5 the moment at the i+ and i stations can be written as

$$M_{i+1} = \sum_{j=0}^{i} \omega^2 m_j y_j (r_j - r_{i+1}) + \sum_{j=0}^{i+1} \omega^2 H_j \alpha_j - \sum_{j=0}^{i} \Omega^2 m_j r_j (y_j - y_{i+1})$$

$$M_i = \sum_{j=0}^{i-1} \omega^2 m_j y_j (r_j - r_i) + \sum_{j=0}^{i} \omega^2 H_j \alpha_j - \sum_{j=0}^{i-1} \Omega^2 m_j r_j (y_j - y_i) \qquad (11a,b)$$

Subtracting M_i from M_{i+1} yields

$$M_{i+1} - M_i = \omega^2 m_i y_i (r_i - r_{i+1}) + \sum_{j=0}^{i-1} \omega^2 m_j y_j (r_i - r_{i+1}) + \omega^2 H_{i+1} \alpha_{i+1}$$

$$- \Omega^2 m_i r_i (y_i - y_{i+1}) - \sum_{j=0}^{i-1} \Omega^2 m_j r_j (y_i - y_{i+1})$$

Introducing the relations

$$l_i = r_i - r_{i+1} \qquad ; \qquad a_i = \sum_{j=0}^{i} m_j r_j \qquad (12)$$

we obtain

$$M_{i+1} - M_i = \omega^2 l_i \sum_{j=0}^{i} m_j y_j + \omega^2 H_{i+1}\alpha_{i+1} - \Omega^2 a_i (y_i - y_{i+1}) \qquad (13)$$

From (7b) we can write

$$\omega^2 \sum_{j=0}^{i} m_j y_j = S_i + \alpha_i a_i \Omega^2$$

which introduced into (13) along with (4) and (5) results in

$$M_{i+1} - M_i = l_i\left[S_i + \alpha_i a_i \Omega^2\right] + \omega^2 H_{i+1}\left[-V_{F_i} S_i - V_{M_i} M_i + \alpha_i\right]$$
$$+ \Omega^2 a_i \left[D_{F_i} S_i + D_{M_i} M_i - l_i \alpha_i\right]$$

$$\boxed{M_{i+1} = \left[l_i - \omega^2 H_{i+1} V_{F_i} + \Omega^2 a_i D_{F_i}\right] S_i + \left[1 - \omega^2 H_{i+1} V_{M_i} + \Omega^2 a_i D_{M_i}\right] M_i + \left[\omega^2 H_{i+1}\right]\alpha_i} \qquad (14)$$

Equations (4), (5), (10) and (14) express the shear, moment, slope and deflection at station i+1 in terms of the same quantities at station i. These equations then provide the means of expressing the conditions at one end of the rotor blade in terms of the conditions at the other end. In order to demonstrate the method it is profitable to use the concise notation of matrix theory. Let us rewrite these four equations as

$$\left.\begin{aligned}
S_{i+1} &= {}_ia_{11} S_i + {}_ia_{12} M_i + {}_ia_{13}\alpha_i + {}_ia_{14} y_i \\
M_{i+1} &= {}_ia_{21} S_i + {}_ia_{22} M_i + {}_ia_{23}\alpha_i + {}_ia_{24} y_i \\
\alpha_{i+1} &= {}_ia_{31} S_i + {}_ia_{32} M_i + {}_ia_{33}\alpha_i + {}_ia_{34} y_i \\
y_{i+1} &= {}_ia_{41} S_i + {}_ia_{42} M_i + {}_ia_{43}\alpha_i + {}_ia_{44} y_i
\end{aligned}\right\} \qquad (15)$$

where ${}_ia_{jk}$ are defined as

$$
\left.
\begin{aligned}
{}_i a_{11} &= 1 + \omega^2 m_{i+1} D_{F_i} + \Omega^2 a_{i+1} V_{F_i} \\
{}_i a_{12} &= \omega^2 m_{i+1} D_{M_i} + \Omega^2 a_{i+1} V_{M_i} \\
{}_i a_{13} &= -\omega^2 m_{i+1} l_i - \Omega^2 m_{i+1} h_{i+1} \\
{}_i a_{14} &= \omega^2 m_{i+1} \\[6pt]
{}_i a_{21} &= l_i - \omega^2 H_{i+1} V_{F_i} + \Omega^2 a_i D_{F_i} \\
{}_i a_{22} &= 1 - \omega^2 H_{i+1} V_{M_i} + \Omega^2 a_i D_{M_i} \\
{}_i a_{23} &= \omega^2 H_{i+1} \\
{}_i a_{24} &= 0 \\[6pt]
{}_i a_{31} &= -V_{F_i} \\
{}_i a_{32} &= -V_{M_i} \\
{}_i a_{33} &= 1 \\
{}_i a_{34} &= 0 \\[6pt]
{}_i a_{41} &= D_{F_i} \\
{}_i a_{42} &= D_{M_i} \\
{}_i a_{43} &= -l_i \\
{}_i a_{44} &= 1
\end{aligned}
\right\} \quad (16)
$$

In matrix notation equation (15) can be written

$$
\begin{Bmatrix} S_{i+1} \\ M_{i+1} \\ \alpha_{i+1} \\ y_{i+1} \end{Bmatrix}
=
\begin{bmatrix}
{}_i a_{11} & {}_i a_{12} & {}_i a_{13} & {}_i a_{14} \\
{}_i a_{21} & {}_i a_{22} & {}_i a_{23} & {}_i a_{24} \\
{}_i a_{31} & {}_i a_{32} & {}_i a_{33} & {}_i a_{34} \\
{}_i a_{41} & {}_i a_{42} & {}_i a_{43} & {}_i a_{44}
\end{bmatrix}
\begin{Bmatrix} S_i \\ M_i \\ \alpha_i \\ y_i \end{Bmatrix}
\quad (17)
$$

and the notation can be further shortened to

$$C_{i+1} = A_i C_i \tag{18}$$

where C stands for the column matrix and A stands for the square matrix. Applying (18) repeatedly we can express the shear, moment, slope and deflection at the root of the blade in terms of the same quantities at the tip. For example.

$$C_1 = A_0 C_0$$
$$C_2 = A_1 C_1 = A_1 A_0 C_0$$
$$C_3 = A_2 C_2 = A_2 A_1 A_0 C_0$$
$$\vdots$$
$$C_n = A_{n-1} C_{n-1} = A_{n-1} \cdots A_1 A_0 C_0$$
$$C_R = A_n C_n = A_n A_{n-1} \cdots A_1 A_0 C_0$$

where C_R is the column matrix associated with the root of the blade and C_0 the column matrix at the tip. If we define the product of the $n+1$ square matrices A_i to be B, we can write

$$B = A_n A_{n-1} \cdots A_1 A_0 = \begin{bmatrix} b_{11} & b_{12} & b_{13} & b_{14} \\ b_{21} & b_{22} & b_{23} & b_{24} \\ b_{31} & b_{32} & b_{33} & b_{34} \\ b_{41} & b_{42} & b_{43} & b_{44} \end{bmatrix} \tag{19}$$

$$C_R = B\, C_0 \tag{20}$$

Writing (20) in expanded form we have

$$\left.\begin{aligned} S_R &= b_{11} S_0 + b_{12} M_0 + b_{13} \alpha_0 + b_{14} y_0 \\ M_R &= b_{21} S_0 + b_{22} M_0 + b_{23} \alpha_0 + b_{24} y_0 \\ \alpha_R &= b_{31} S_0 + b_{32} M_0 + b_{33} \alpha_0 + b_{34} y_0 \\ y_R &= b_{41} S_0 + b_{42} M_0 + b_{43} \alpha_0 + b_{44} y_0 \end{aligned}\right\} \tag{21}$$

Boundary Conditions:

If we normalize the tip deflection to one, then the usual boundary conditions for a helicopter rotor blade are for the tip of the blade

$$S_0 = 0$$
$$M_0 = 0$$
$$\alpha_0$$
$$y_0 = 1$$

and for the root of the blade

$$\left.\begin{array}{l} S_R \\ M_R = 0 \\ \alpha_R \\ y_R = 0 \end{array}\right\} \text{hinged blade} \qquad \left.\begin{array}{l} S_R \\ M_R \\ \alpha_R = 0 \\ y_R = 0 \end{array}\right\} \text{for the fixed blade}$$

As for example if we substitute the tip conditions into (21) and solve for the root conditions we obtain

$$\left.\begin{array}{l} M_R = b_{23}\alpha_0 + b_{24} \\ \alpha_R = b_{33}\alpha_0 + b_{34} \\ y_R = b_{43}\alpha_0 + b_{44} \end{array}\right\} \qquad (22)$$

For a hinged rotor blade M_R and y_R should both be zero. Setting $y_R = 0$ and solving for α_0 and then substituting into the expression for M_R we obtain

$$y_R = 0 = b_{43}\alpha_0 + b_{44}$$

$$\alpha_0 = -\frac{b_{44}}{b_{43}} \qquad (23)$$

$$M_R = b_{23}\alpha_0 + b_{24}$$

$$M_R = b_{24} - b_{23}\frac{b_{44}}{b_{43}} \qquad (24)$$

The steps in the determination of the natural frequencies and mode shapes are the following. Assume a value of ω^2 and compute all A_i. Then, multiply these four by four matrices to obtain the product matrix B. From B compute the root moment

$$M_R = b_{24} - b_{23}\,\frac{b_{44}}{b_{43}} \tag{25}$$

A plot of M_R versus the assumed natural frequency will appear as follows

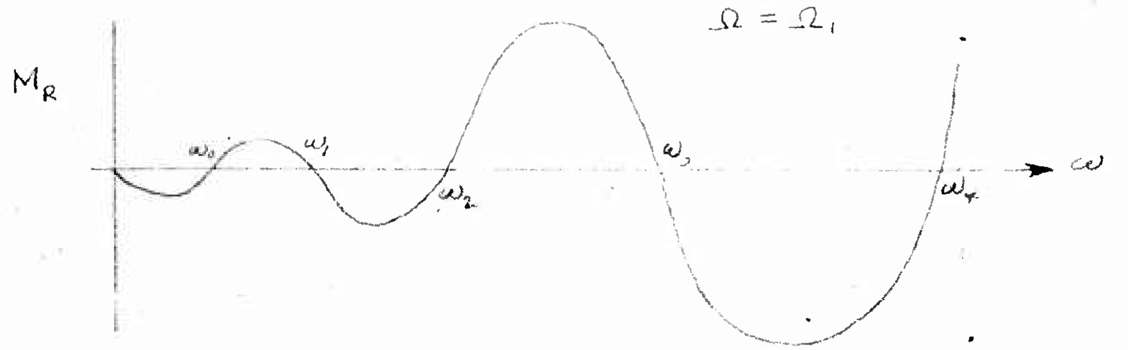

When $M_R = 0$ the boundary conditions will be satisfied and the natural frequency will be determined.

ω_0 = rigid body mode $(\omega_0 \cong \Omega)$
ω_1 = first elastic mode $(\omega_0 \cong 2.5\Omega - 3.5\Omega)$

When, say ω_1 has been determined α_0 can be calculated from (24). Then with the tip conditions known, the shear, moment, slope and deflection at each station can be determined using the relations

$$\begin{Bmatrix} S_1 \\ M_1 \\ \alpha_1 \\ y_1 \end{Bmatrix} = \begin{bmatrix} A \end{bmatrix}_0 \begin{Bmatrix} S_0 = 0 \\ M_0 = 0 \\ \alpha_0 \\ y_0 = 1 \end{Bmatrix}$$

$$C_1 = A_0 C_0$$
$$C_2 = A_1 C_1$$
$$C_3 = A_2 C_2$$
$$\vdots \qquad \vdots$$
$$C_R = A_n C_n$$

The routine is identical in the case of a fixed rotor blade. However in this case α_R can be plotted against assumed natural frequency ω where

$$\alpha_R = b_{34} - b_{33}\frac{b_{44}}{b_{43}} \qquad (26)$$

Chordwise Vibrations

The only difference between flapwise vibrations and chordwise vibrations is in the effect of the centrifugal forces. Figure 6 shows the external forces acting on the rotating blade when it is vibrating in a chordwise mode. This Figure should be compared with Figure 5.

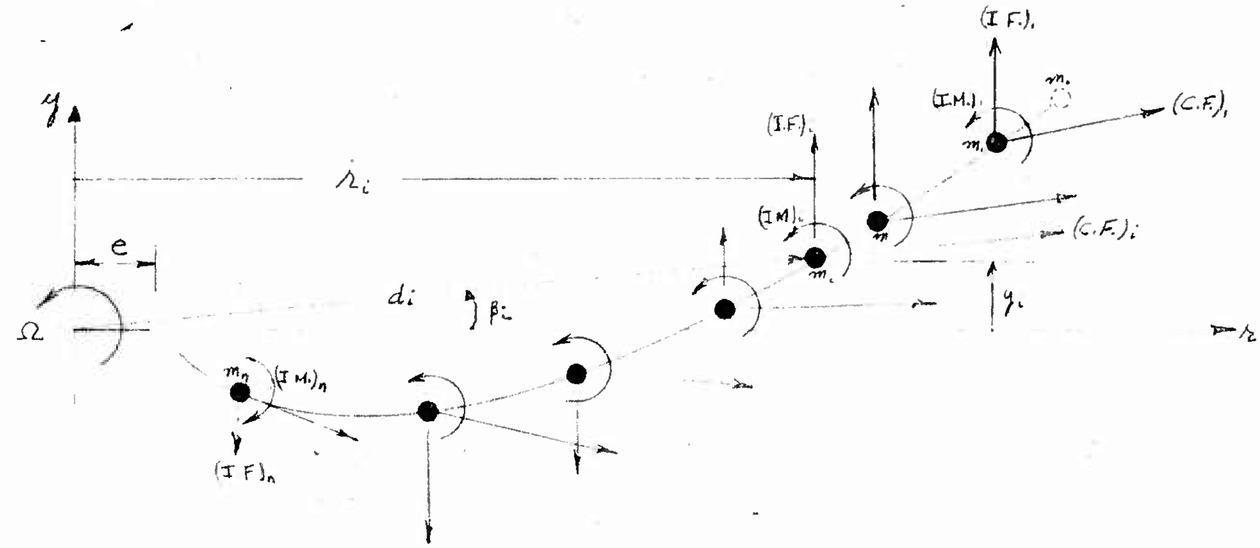

FIGURE 6 EXTERNAL FORCES ACTING ON BLADE

From Figure 6 observe that there is a component of the centrifugal force acting in the direction of the inertia force. Let us resolve the centrifugal force into a component in the direction of the inertia force (along y) and a component along r.

The forces acting on the i^{th} mass are

$$(I.F.)_i = m_i y_i \omega^2$$
$$(C.F.)_i = m_i d_i \Omega^2$$

Resolving the centrifugal force into the two components along y and r we have

$$\text{along } y = m_i d_i \Omega^2 \sin\beta_i = m_i d_i \Omega^2 \left(\frac{y_i}{d_i}\right) = m_i y_i \Omega^2$$
$$\text{along } r = m_i d_i \Omega^2 \cos\beta_i = m_i d_i \Omega^2 \left(\frac{r_i}{d_i}\right) = m_i r_i \Omega^2$$

If we define $\bar{\omega}$ to be

$$\bar{\omega}^2 = \omega^2 + \Omega^2 \qquad (27)$$

then the force acting on the i^{th} mass along y becomes

$$m_i y_i \bar{\omega}^2$$

and the force acting on the i^{th} mass along r was

$$m_i r_i \Omega^2$$

Hence we see that this case is identical with the flapwise case if we replace the flapwise ω^2 by $\bar{\omega}^2$.

To summarize we can say that in determining the natural frequency of the rotor blade for chordwise vibrations one should treat the problem as a flapwise vibration problem using the chordwise stiffness properties. Then when the frequencies have been determined for flapwise bending, the chordwise frequencies are determined from the relation

$$\omega^2_{chordwise} = \omega^2_{flapwise} - \Omega^2 \qquad (28)$$

UNCLASSIFIED

UNCLASSIFIED